

## Multiple four-wave mixing self-stability in optical fibers

Xueming Liu,\* Xiaoqun Zhou, and Chao Lu

*Institute for Infocomm Research, Unit 230, Innovation Centre, Block 2, 18 Nanyang Drive, Singapore 637723*

(Received 10 February 2005; revised manuscript received 28 March 2005; published 14 July 2005)

The self-stability of multiple four-wave mixing (FWM) processes in the optical fibers is studied both theoretically and experimentally. The coupled-mode equations for the complex amplitudes of four waves are derived. The nonlinear interaction between four optical fields involves a single nondegenerate and two degenerate FWM processes in the third-order nonlinear mixings. The proposed models are compared to the conventional coupled-mode theory of FWM processes and are proven by the experiments. The energy conservation of four waves is achieved, and the power flow relationship between two pump waves and two created waves is obtained. The analytic solutions reveal the self-stability mechanism of multiple FWM processes. The self-stability prediction is experimentally testified by using a kind of photonic-crystal fiber, and such excellence can be applied to achieve dual-wavelength erbium-doped fiber lasers with the excellent uniformity and stability.

DOI: [10.1103/PhysRevA.72.013811](https://doi.org/10.1103/PhysRevA.72.013811)

PACS number(s): 42.65.Hw, 42.55.Tv, 42.55.Wd, 42.81.Gs

### I. INTRODUCTION

The third-order optical nonlinear effects such as third-harmonic generation and four-wave mixing (FWM) involve the generation of new frequencies [1,2]. FWM is one of main nonlinear optical processes in single-mode optical fiber [3], and leads to many applications such as parametric amplification, wavelength conversion, and oscillator [4–6]. The existence and efficiency of generating new frequencies by FWM need special efforts to achieve phase matching [7], which is determined by the dispersive properties of materials. In conventional optical fibers, the dispersion profile is well approximated by a group velocity dispersion [6,8].

Recently, photonic-crystal fibers (PCFs) have attracted a lot of interest because of their unusual optical properties and their potential applications [9–12]. In comparison with conventional optical fibers, PCFs can provide tiny core areas and dispersion characteristics that can be strongly modified. As a result, the significant FWMs can occur at relatively low peak powers and over short propagation distances, and such processes can be possible in a much greater frequency range. To show the dispersion difference between conventional fibers and PCFs, Fig. 1 illustrates the relationship of dispersion parameter  $D$  versus wavelength, where Fig. 1(a) is for the typical single-mode fiber [6] and Fig. 1(b) is for a kind of PCF [13]. At the same time, such PCF provides the nonlinearity coefficient  $\gamma$  of  $\sim 11 \text{ W}^{-1} \text{ km}^{-1}$ , while  $\gamma$  of the conventional fiber is  $\sim 1.3 \text{ W}^{-1} \text{ km}^{-1}$  [6]. Therefore, the advent of PCF with the high  $\gamma$  value and the “engineered” dispersion profiles suggests that there is the opportunity to develop a family of nonlinear effects that cannot be observed in standard optical fibers [8,14].

In 1974, the phase-matched nonlinear mixing in the silica fiber was observed [15]. The typical coupled-mode equations for nondegenerate or degenerate FWMs can be applied to explain most experiments in the conventional fibers [6,16]. These theories had generally been concerned with a single

degenerate or nondegenerate FWM process. In 1991, Thompson *et al.* had proposed and derived the coupled-mode equations for multiple FWM processes [17]. However, all of these theories have some difficulty in explaining a feature of

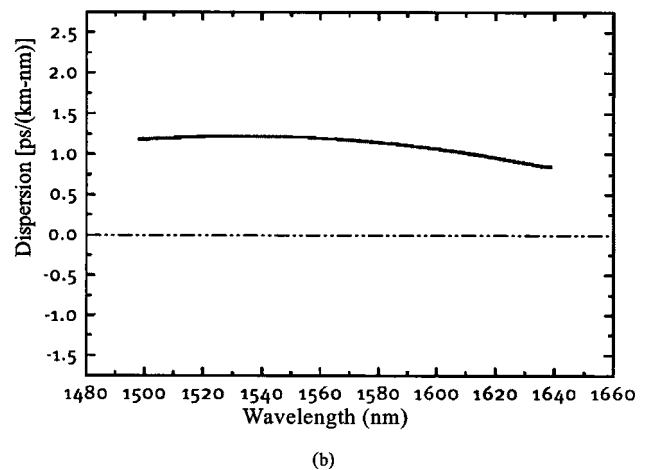
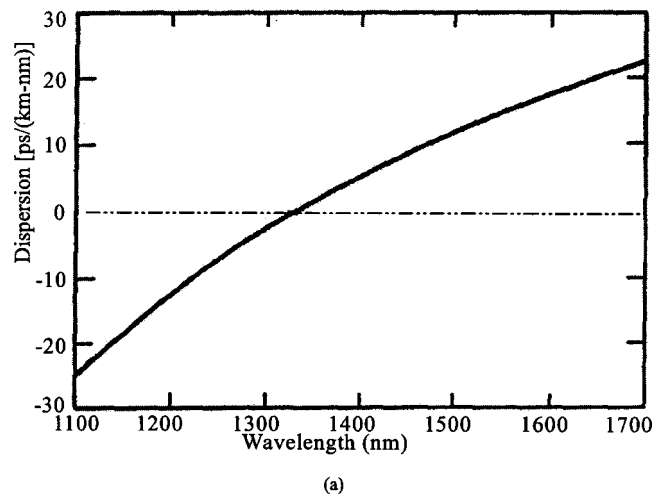


FIG. 1. Dispersion parameter  $D$  with wavelength: (a) for conventional single-mode fibers and (b) for a kind of PCF.

\*Email address: liuxueming72@yahoo.com

FWM in PCFs in our experiments. This work has proposed a model for multiple FWM processes where the self-stability function of such FWM processes is revealed. Such phenomenon is experimentally verified and can find important applications, such as fiber lasers.

## II. DERIVATION FOR COMPLEX AMPLITUDE PROPAGATION EQUATIONS

The propagation equations for describing self-phase-modulation, cross-phase-modulation, and FWM can be derived from Maxwell's equations by including the proper terms of the nonlinear polarization of the fiber medium [17]. The nonlinear wave equation can be expressed as

$$\nabla^2 \mathbf{E} - \frac{n_0^2}{c^2} \frac{\partial^2 \mathbf{E}}{\partial t^2} = \mu_0 \frac{\partial^2 \mathbf{P}_{\text{NL}}}{\partial t^2}, \quad (1a)$$

where  $n_0 = (1 + \chi^{(1)})^{1/2}$ ,  $\chi^{(1)}$  is the linear susceptibility of the dielectric medium, and

$$\mathbf{P}_{\text{NL}} = \varepsilon_0 \chi^{(3)} : \mathbf{E} \mathbf{E} \mathbf{E}. \quad (1b)$$

Taking into account four optical waves vibrating at frequencies  $\omega_1$ ,  $\omega_2$ ,  $\omega_3$ , and  $\omega_4$  and linearly polarized along the same axis  $x$ , the total electric field of the guided modes can be expressed as the superposition of individual normal mode, i.e.,

$$\mathbf{E} = \frac{1}{2} \hat{x} \sum_{m=1}^4 E_m \exp[i(\beta_m z - \omega_m t)] + c.c., \quad (2)$$

where  $c.c.$  denotes the complex conjugate,  $\hat{x}$  is the polarization unit vector,  $\beta_m = n_m \omega_m / 2$  is the axial propagation constant and includes material and waveguiding effects in the refractive index  $n_m$ . Substituting Eq. (2) in Eq. (1b), one can achieve [6,17]

$$\begin{aligned} \mathbf{P}_{\text{NL}} &= \frac{1}{2} \hat{x} \sum_{j=1}^4 P_{\text{NL},j} \exp[i(\beta_j z - \omega_j t)] + c.c. \\ &= \frac{1}{8} \varepsilon_0 \chi^{(3)} \hat{x} \sum_{k,l,m} E_k E_l E_m \exp[i(\xi_k + \xi_l + \xi_m)], \end{aligned} \quad (3)$$

where  $\xi_k = \beta_k z - \omega_k t$  and  $k, l, m = 1, 2, 3, 4$  and  $1^*, 2^*, 3^*, 4^*$ . The raised asterisk denotes that the complex conjugate is to be taken. Equation (3) has a large number of terms involving the products of three electric fields. For example,  $P_{\text{NL},1}$  can be expressed as

$$\begin{aligned} P_{\text{NL},1} &= \frac{3}{4} \varepsilon_0 \chi^{(3)} \left[ \left( |E_1|^2 + 2 \sum_{j \neq 1} |E_j|^2 \right) E_1 + 2E_2 E_3 E_4 \exp(i\theta_0) \right. \\ &\quad + 2E_1^* E_2 E_3 \exp(i\theta_1) + E_4^* E_2^2 \exp(-i\theta_2) \\ &\quad \left. + 2E_2^* E_3 E_4 \exp(i\theta_3) + \dots \right], \end{aligned} \quad (4a)$$

$$\begin{aligned} \theta_0 &= [\beta(\omega_2) + \beta(\omega_3) + \beta(\omega_4) - \beta(\omega_1)]z \\ &\quad - (\omega_2 + \omega_3 + \omega_4 - \omega_1)t, \end{aligned} \quad (4b)$$

$$\theta_1 = [\beta(\omega_2) + \beta(\omega_3) - 2\beta(\omega_1)]z - (\omega_2 + \omega_3 - 2\omega_1)t, \quad (4c)$$

$$\theta_2 = [\beta(\omega_1) + \beta(\omega_4) - 2\beta(\omega_2)]z - (\omega_1 + \omega_4 - 2\omega_2)t, \quad (4d)$$

$$\begin{aligned} \theta_3 &= [\beta(\omega_3) + \beta(\omega_4) - \beta(\omega_1) - \beta(\omega_2)]z \\ &\quad - (\omega_3 + \omega_4 - \omega_1 - \omega_2)t. \end{aligned} \quad (4e)$$

Here,  $\theta_0$ ,  $\theta_1$ ,  $\theta_2$ , and  $\theta_3$  are responsible for the phenomena of third-harmonic generation, two degenerate FWMs, and a nondegenerate FWM, respectively.

In this work, the total FWM processes include two degenerate processes given by  $2\omega_1 = \omega_2 + \omega_3$  [corresponding to Eq. (4c)] and  $2\omega_2 = \omega_1 + \omega_4$  [corresponding to Eq. (4d)] and one nondegenerate process given by  $\omega_1 + \omega_2 = \omega_3 + \omega_4$  [corresponding to Eq. (4e)]. Although Eq. (3) includes many terms, such as third-harmonic generation [e.g., Eq. (4b)], significant FWMs occur only if the frequencies perfectly match and the phase mismatch nearly vanishes. Under the assumption of quasi-continuous-wave conditions, the time derivatives can be replaced by the quantity  $-i\omega$ . From Eq. (3), we can obtain

$$\begin{aligned} \mu_0 \frac{\partial^2 \mathbf{P}_{\text{NL}}(\omega_1)}{\partial t^2} &= -\frac{3\chi^{(3)}\omega_1^2}{8c^2} \hat{x} \left[ \left( |E_1|^2 + 2 \sum_{j \neq 1} |E_j|^2 \right) E_1 \right. \\ &\quad + 2E_1^* E_2 E_3 e^{i\Delta\beta_1 z} + E_4^* E_2^2 e^{-i\Delta\beta_2 z} \\ &\quad \left. + 2E_2^* E_3 E_4 e^{i\Delta\beta_3 z} \right] e^{i(\beta_1 z - \omega_1 t)}, \end{aligned} \quad (5a)$$

$$\begin{aligned} \mu_0 \frac{\partial^2 \mathbf{P}_{\text{NL}}(\omega_2)}{\partial t^2} &= -\frac{3\chi^{(3)}\omega_2^2}{8c^2} \hat{x} \left[ \left( |E_2|^2 + 2 \sum_{j \neq 2} |E_j|^2 \right) E_2 \right. \\ &\quad + 2E_2^* E_1 E_4 e^{i\Delta\beta_2 z} + E_3^* E_1^2 e^{-i\Delta\beta_1 z} \\ &\quad \left. + 2E_1^* E_3 E_4 e^{i\Delta\beta_3 z} \right] e^{i(\beta_2 z - \omega_2 t)}, \end{aligned} \quad (5b)$$

$$\begin{aligned} \mu_0 \frac{\partial^2 \mathbf{P}_{\text{NL}}(\omega_3)}{\partial t^2} &= -\frac{3\chi^{(3)}\omega_3^2}{8c^2} \hat{x} \left[ \left( |E_3|^2 + 2 \sum_{j \neq 3} |E_j|^2 \right) E_3 \right. \\ &\quad + E_2^* E_1^2 e^{-i\Delta\beta_1 z} + 2E_4^* E_1 E_2 e^{-i\Delta\beta_3 z} \left. \right] e^{i(\beta_3 z - \omega_3 t)}, \end{aligned} \quad (5c)$$

$$\begin{aligned} \mu_0 \frac{\partial^2 \mathbf{P}_{\text{NL}}(\omega_4)}{\partial t^2} &= -\frac{3\chi^{(3)}\omega_4^2}{8c^2} \hat{x} \left[ \left( |E_4|^2 + 2 \sum_{j \neq 4} |E_j|^2 \right) E_4 \right. \\ &\quad \left. + E_1^* E_2^2 e^{-i\Delta\beta_2 z} + 2E_3^* E_1 E_2 e^{-i\Delta\beta_3 z} \right] e^{i(\beta_4 z - \omega_4 t)}, \end{aligned} \quad (5d)$$

where  $\Delta\beta_1 = \beta(\omega_2) + \beta(\omega_3) - 2\beta(\omega_1)$ ,  $\Delta\beta_2 = \beta(\omega_1) + \beta(\omega_4) - 2\beta(\omega_2)$  and  $\Delta\beta_3 = \beta(\omega_3) + \beta(\omega_4) - \beta(\omega_1) - \beta(\omega_2)$ . Because of  $\Delta\beta_3 = \Delta\beta_1 + \Delta\beta_2$ , only two independent resonant conditions should be satisfied simultaneously in Eq. (5).

The field amplitudes can be separated into transverse and longitudinal parts, i.e., the product of functions of the trans-

verse coordinates  $r$  and  $\phi$  and the axial coordinate  $z$  [6,17],

$$E_j(\mathbf{r}) = A_j(z)\psi_j(r, \phi)/N_j \quad (j = 1 \text{ to } 4), \quad (6)$$

where  $|A_j|^2$  is equal to the power  $P_j$  (i.e.,  $P_j = |A_j|^2$ ),  $\psi_j(r, \phi)$  is the spatial distribution of the fiber mode in which the  $j$ th field propagates inside the fiber, and

$$N_j^2 = \frac{1}{2} \varepsilon_0 n_0 c \int \int |\psi_j|^2 r dr d\phi \quad (j = 1 \text{ to } 4). \quad (7)$$

In the slowly varying envelope approximation and under the assumption that the transverse modes remain essentially unperturbed by the nonlinearity, the left-hand side of Eq. (1a) can be simplified as [17]

$$\begin{aligned} \nabla^2 \mathbf{E}(\omega_j) - \frac{n_0^2}{c^2} \frac{\partial^2 \mathbf{E}(\omega_j)}{\partial t^2} &\approx i \beta_j \frac{\psi_j}{N_j} \frac{\partial A_j}{\partial z} \hat{x} \exp[i(\beta_j z - \omega_j t)] \\ &\times (j = 1 \text{ to } 4). \end{aligned} \quad (8)$$

After some manipulation from Eqs. (1), and (5)–(8), we can achieve

$$\begin{aligned} \frac{\partial A_1}{\partial z} &= i \gamma_1 \left[ \left( |A_1|^2 + 2 \sum_{j(\neq 1)} |A_j|^2 \right) A_1 + 2A_1^* A_2 A_3 \exp(i\Delta\beta_1 z) \right. \\ &\quad \left. + A_4^* A_2^2 \exp(-i\Delta\beta_2 z) + 2A_2^* A_3 A_4 \exp(i\Delta\beta_3 z) \right], \end{aligned} \quad (9a)$$

$$\begin{aligned} \frac{\partial A_2}{\partial z} &= i \gamma_2 \left[ \left( |A_2|^2 + 2 \sum_{j(\neq 2)} |A_j|^2 \right) A_2 + 2A_2^* A_1 A_4 \exp(i\Delta\beta_2 z) \right. \\ &\quad \left. + A_3^* A_1^2 \exp(-i\Delta\beta_1 z) + 2A_1^* A_3 A_4 \exp(i\Delta\beta_3 z) \right], \end{aligned} \quad (9b)$$

$$\begin{aligned} \frac{\partial A_3}{\partial z} &= i \gamma_3 \left[ \left( |A_3|^2 + 2 \sum_{j(\neq 3)} |A_j|^2 \right) A_3 + A_2^* A_1^2 \exp(-i\Delta\beta_1 z) \right. \\ &\quad \left. + 2A_4^* A_1 A_2 \exp(-i\Delta\beta_3 z) \right], \end{aligned} \quad (9c)$$

$$\begin{aligned} \frac{\partial A_4}{\partial z} &= i \gamma_4 \left[ \left( |A_4|^2 + 2 \sum_{j(\neq 4)} |A_j|^2 \right) A_4 + A_1^* A_2^2 \exp(-i\Delta\beta_2 z) \right. \\ &\quad \left. + 2A_3^* A_1 A_2 \exp(-i\Delta\beta_3 z) \right], \end{aligned} \quad (9d)$$

where the nonlinearity coefficient  $\gamma_j$  is defined as

$$\gamma_j \equiv n_2^j \omega_j / (c A_{\text{eff}}) \quad (j = 1 \text{ to } 4). \quad (10)$$

$n_2^j$  and  $A_{\text{eff}}$  are given by

$$n_2^j \equiv 3\chi^{(3)} / (4\varepsilon_0 c n_0^2), \quad (11a)$$

$$A_{\text{eff}} \equiv \left( \int \int |\psi_j|^2 r dr d\phi \right)^2 / \int \int |\psi_j|^4 r dr d\phi \quad (j = 1 \text{ to } 4). \quad (11b)$$

Usually, the relatively small differences in optical frequencies of four waves can be ignored and then  $\gamma_j$  can be the average value  $\gamma$ .

In Eq. (9), it evolved into a single nondegenerate FWM process (i.e.,  $\omega_1 + \omega_2 = \omega_3 + \omega_4$ ) and two degenerate FWM processes (i.e.,  $2\omega_1 = \omega_2 + \omega_3$  and  $2\omega_2 = \omega_1 + \omega_4$ ). However, the conventional coupled-mode equations for FWM processes are only referred to either a nondegenerate FWM or a degenerate FWM process [6]. Their detailed relationship and difference are shown in Sec. V. Therefore, our model is a self-consistent system for the complex amplitudes of the four fields, which is associated with products of electric-field amplitudes in the polarization expansion such as  $2E_{\omega_1}^* E_{\omega_2} E_{\omega_3}$ ,  $2E_{\omega_2}^* E_{\omega_1} E_{\omega_4}$ ,  $2E_{\omega_2}^* E_{\omega_3} E_{\omega_4}$ ,  $E_{\omega_2}^2 E_{\omega_4}^*$ ,  $E_{\omega_1}^2 E_{\omega_3}^*$ ,  $E_{\omega_1}^* E_{\omega_2}^*$ , and so on.

### III. RESULTS AND DISCUSSIONS

Let  $A_j = \sqrt{P_j} \exp(i\varphi_j)$  for  $j \in \{1, 2, 3, 4\}$ , and substitute it into Eq. (9). After some manipulation, we can recast Eq. (9) into equivalent real equations:

$$\begin{aligned} \frac{\partial P_1}{\partial z} &= \gamma (2P_2 \sqrt{P_1 P_4} \sin \vartheta_2 - 4P_1 \sqrt{P_2 P_3} \sin \vartheta_1 \\ &\quad - 4\sqrt{P_1 P_2 P_3 P_4} \sin \vartheta_3), \end{aligned} \quad (12a)$$

$$\begin{aligned} \frac{\partial P_2}{\partial z} &= \gamma (2P_1 \sqrt{P_2 P_3} \sin \vartheta_1 - 4P_2 \sqrt{P_1 P_4} \sin \vartheta_2 \\ &\quad - 4\sqrt{P_1 P_2 P_3 P_4} \sin \vartheta_3), \end{aligned} \quad (12b)$$

$$\begin{aligned} \frac{\partial P_3}{\partial z} &= \gamma (2P_1 \sqrt{P_2 P_3} \sin \vartheta_1 + 4\sqrt{P_1 P_2 P_3 P_4} \sin \vartheta_3), \end{aligned} \quad (12c)$$

$$\begin{aligned} \frac{\partial P_4}{\partial z} &= \gamma (2P_2 \sqrt{P_1 P_4} \sin \vartheta_2 + 4\sqrt{P_1 P_2 P_3 P_4} \sin \vartheta_3), \end{aligned} \quad (12d)$$

where  $\vartheta_1 = \Delta\beta_1 z + \varphi_2 + \varphi_3 - 2\varphi_1$ ,  $\vartheta_2 = \Delta\beta_2 z + \varphi_1 + \varphi_4 - 2\varphi_2$ , and  $\vartheta_3 = \Delta\beta_3 z + \varphi_3 + \varphi_4 - \varphi_1 - \varphi_2$ .

From Eq. (12), one can easily verify that the power exchanges among four waves depend on their powers and the signs of  $\sin \vartheta_1$ ,  $\sin \vartheta_2$ , and  $\sin \vartheta_3$ . It is worth noting that there exist the power flows between two pump waves (i.e.,  $\omega_1$  and  $\omega_2$ ) in our model. However, in the conventional coupled-mode equations of nondegenerate FWM process [i.e., Eq. (27)], two pump waves do not exchange energy during the total nonlinear mixings.

It is shown that Eq. (12) displays power conservation, i.e.,

$$\begin{aligned} \frac{\partial (P_1 + P_2 + P_3 + P_4)}{\partial z} &= 0 \quad \text{or} \\ P_1(z) + P_2(z) + P_3(z) + P_4(z) &= \text{constant}. \end{aligned} \quad (13)$$

Equation (13) demonstrates the famous Manley–Rowe relations. Besides conserving total power in Eq. (13), an additional invariant is covered in the system of Eq. (12), i.e.,

$$\frac{\partial(P_1 - P_2)}{\partial z} = -3 \frac{\partial(P_3 - P_4)}{\partial z}. \quad (14)$$

Equation (14) shows that power flow between two pump waves of  $\omega_1$  and  $\omega_2$  is thrice larger than that between two created waves of  $\omega_4$  and  $\omega_3$  at any propagating distance along the fiber. The invariance in Eq. (14) physically represents conservation between the power exchange of two pump waves and that of two sidebands. The physical reasoning can be explained as follows.

During two degenerate FWM processes of  $2\omega_1 = \omega_2 + \omega_3$  and  $2\omega_2 = \omega_1 + \omega_4$  (because two pump waves in the nondegenerate FWM process do not transfer energy, this kind of process is ignored here), two photons of frequency  $\omega_1$  (or  $\omega_2$ ) are annihilated in order to create one photon of frequency  $\omega_2$  (or  $\omega_1$ ) and another photon of frequency  $\omega_3$  (or  $\omega_4$ ). Then, the energy flow between three photon  $\omega_1$  and  $\omega_2$  is to produce that between one photon  $\omega_3$  and  $\omega_4$ , i.e.,  $3(\omega_1 - \omega_2) = \omega_3 - \omega_4$ . As a result, in the total interacting processes, the photon-exchanging number of  $\omega_1$  and  $\omega_2$  is as three times large as that of  $\omega_3$  and  $\omega_4$ . Taking into account the fact of  $\omega_1 \approx \omega_2 \approx \omega_3 \approx \omega_4$ , the total energy exchange between two pumps is three times more than that between two created waves, i.e., Eq. (14).

In this work, we focus on the conditions that the powers of frequencies  $\omega_1$  and  $\omega_2$  are great larger than those of frequencies  $\omega_3$  and  $\omega_4$ , and that the former keep the undepleted approximation during the nonlinear interaction in the total FWM processes, i.e.,

$$|A_1|, |A_2| \gg |A_3|, |A_4|, \quad (15a)$$

$$|A_1(z)| = |A_1(0)| \quad \text{and} \quad |A_2(z)| = |A_2(0)|. \quad (15b)$$

Then, Eqs. (9a) and (9b) can be solved as

$$A_1(z) \approx \sqrt{P_1} \exp[i\gamma(P_1 + 2P_2)z + i\varphi_1(0)], \quad (16a)$$

$$A_2(z) \approx \sqrt{P_2} \exp[i\gamma(P_2 + 2P_1)z + i\varphi_2(0)]. \quad (16b)$$

Taking into account Eq. (15) and substituting Eq. (16) into Eqs. (9c) and (9d), we can solve as

$$\begin{aligned} A_3(L) &\approx \int_0^L i\gamma A_2^* A_1^2 \exp(-i\Delta\beta_1 z) dz \\ &= i\gamma P_1 \sqrt{P_2} \exp[2i\varphi_1(0) - i\varphi_2(0)] \\ &\quad \times \frac{\exp[i(3\gamma P_2 - \Delta\beta_1)L] - 1}{i(3\gamma P_2 - \Delta\beta_1)}, \end{aligned} \quad (17a)$$

$$\begin{aligned} A_4(L) &\approx \int_0^L i\gamma A_1^* A_2^2 \exp(-i\Delta\beta_2 z) dz \\ &= i\gamma P_2 \sqrt{P_1} \exp[2i\varphi_2(0) - i\varphi_1(0)] \\ &\quad \times \frac{\exp[i(3\gamma P_1 - \Delta\beta_2)L] - 1}{i(3\gamma P_1 - \Delta\beta_2)}. \end{aligned} \quad (17b)$$

If  $(3\gamma P_1 - \Delta\beta_2)L \rightarrow 0$  and  $(3\gamma P_2 - \Delta\beta_1)L \rightarrow 0$ , from Eq. (17), we can obtain as

$$P_3(L) = \gamma^2 L^2 P_1(0)^2 P_2(0) \quad \text{and} \quad P_4(L) = \gamma^2 L^2 P_2(0)^2 P_1(0). \quad (18)$$

From Eqs. (14) and (18), we can achieve as

$$P_{12}(L) - P_{12}(0) = -3\gamma^2 L^2 P_1(0) P_2(0) [P_1(0) - P_2(0)], \quad (19)$$

where  $P_{12}(z) = P_1(z) - P_2(z)$ . From Eq. (19), it can be seen as follows:

If  $P_1(0) > P_2(0)$ ,  $P_1(0) - P_2(0) > 0$  and  $P_{12}(L) < P_{12}(0)$ . Taking into account Manley-Rowe relations [i.e., Eq. (13)], the power of frequency  $\omega_1$  flows into that of frequency  $\omega_2$  during the FWM processes.

If  $P_2(0) > P_1(0)$ ,  $P_1(0) - P_2(0) < 0$  and  $P_{12}(L) > P_{12}(0)$ , and then the power at  $\omega_2$  flows into that at  $\omega_1$ .

If  $P_2(0) = P_1(0)$ ,  $P_{12}(L) = P_{12}(0)$  and  $P_1(L) = P_2(L)$ . This result shows that the powers at  $\omega_1$  and  $\omega_2$  remain the same during total FWM interaction processes.

The above results reveal the fact that these kinds of multiple FWM processes hold an important unique property of self-stability mechanism, i.e., the energy flow transfers from higher-power wave to lower-power wave with the self-driven function.

With the increase of  $\gamma$ ,  $L$ ,  $P_1(0)$ , and  $P_2(0)$ , the self-stability enhancement for frequencies  $\omega_1$  and  $\omega_2$  is improved on the assistance of two degenerate and one nondegenerate FWM processes.

The greater the difference of  $P_1(0) - P_2(0)$ , the greater the difference of  $P_1(L) - P_2(L)$  (i.e., there is more power flow exchanging from higher to lower power).

#### IV. EXPERIMENTS AND APPLICATIONS

Dual- or multiwavelength erbium-doped fiber (EDF) lasers have caused extensive interest in recent years due to their potential applications, such as wavelength division multiplexer (WDM) systems, fiber sensors, and fiber-optics instrumentation [18,19]. However, because of the large homogeneous linewidth of EDF at room temperature [20,21],

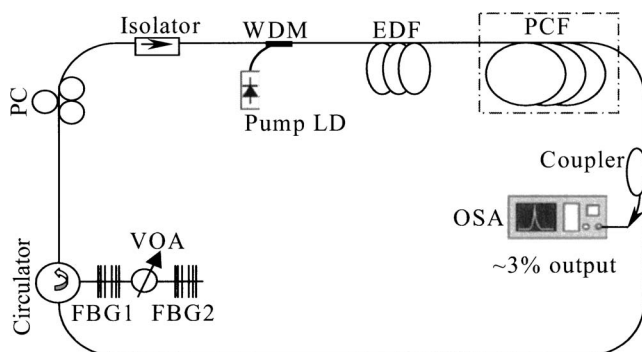


FIG. 2. Experimental setup for testing the self-stability mechanism of multiple FWM processes on the basis of dual-wavelength EDF laser loop. EDF: erbium-doped fiber, VOA: variable optical attenuator, PCF: photonic-crystal fiber, FBG: fiber Bragg grating, PC: polarization controller, WDM: wavelength division multiplexer, and OSA: optical spectra analyzer.

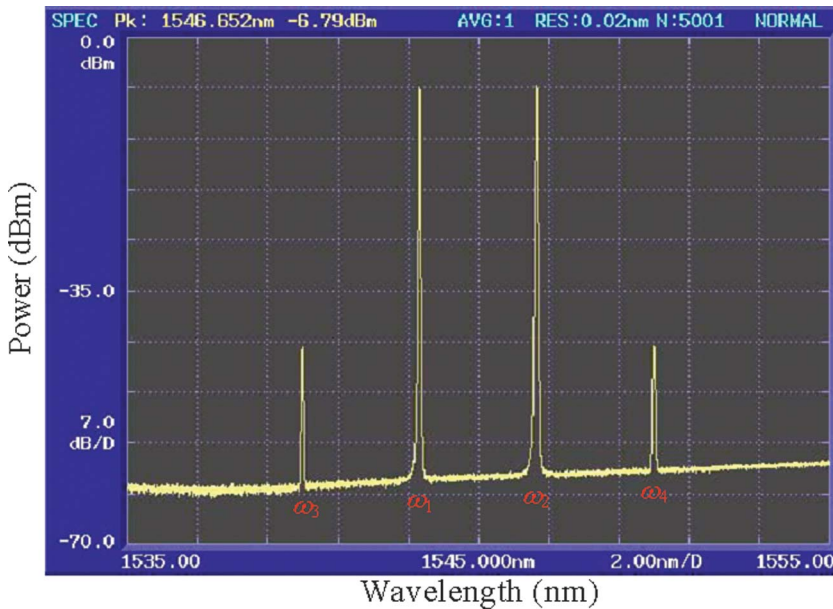


FIG. 3. (Color) Output power spectra on the gain-clamping balances between self-stability effect of multiple FWM processes and mode competition effect of EDF. Pump waves at  $\omega_1$  and  $\omega_2$  are lased by the cavity, and two waves at  $\omega_3$  and  $\omega_4$  are produced by the FWM processes of PCF. Two degenerate FWM processes of  $2\omega_1 = \omega_2 + \omega_3$  and  $2\omega_2 = \omega_1 + \omega_4$  and one nondegenerate FWM process of  $\omega_1 + \omega_2 = \omega_3 + \omega_4$  effectively interacted.

dual- or multiwavelength EDF lasers experience cross-saturation between different wavelengths which cause unstable lasing [19–24]. In order to achieve stable dual-wavelength operation, various techniques, such as two EDFs [24], two filters and attenuators [22] and two overlapping cavities [19], had been employed. Even the EDF was cooled to liquid-nitrogen temperature [19,20].

In this paper, the self-stability function of multiple FWM processes has been experimentally proven on the basis of dual-wavelength EDF lasers. The experimental setup is based on the typical EDF laser loop that is demonstrated in Fig. 2. A 51-m-long high nonlinear PCF with the flat near-zero dispersion causes one nondegenerate and two degenerate FWM processes [13]. The EDF and pump LD of 1480 nm lase two waves of frequencies  $\omega_1$  and  $\omega_2$ . A variable optical attenuator (VOA) is used to adjust the reflection spectra of FBG2. Two Blackman apodization FBG1 and FBG2

are with the central wavelength of 1543.32 nm and 1546.65 nm, and the reflectivity of 59.4% and 99.5%, respectively.

In the conventional EDF cavity without additional techniques or methods, only a single wave can be stably lased [19–24]. Note that the setup in Fig. 2 is a typical EDF cavity if excluding PCF. To suppress the mode competition caused by the homogeneous gain broadening of EDF, introducing self-stability function of multiple FWM processes into the oscillator can produce dual-wavelength EDF lasers with the excellent stability and uniformity. The balance between the self-stability effect of FWM and the mode competition of EDF can cause the gain-clamping function and lead to the dual-wavelength lasing simultaneously.

Figure 3 demonstrates the experimental results on the gain-clamping balances between self-stability effect of FWM and mode competition effect of EDF. Waves of frequencies  $\omega_1$  and  $\omega_2$  are lased by the cavity, and are called pumps. Two

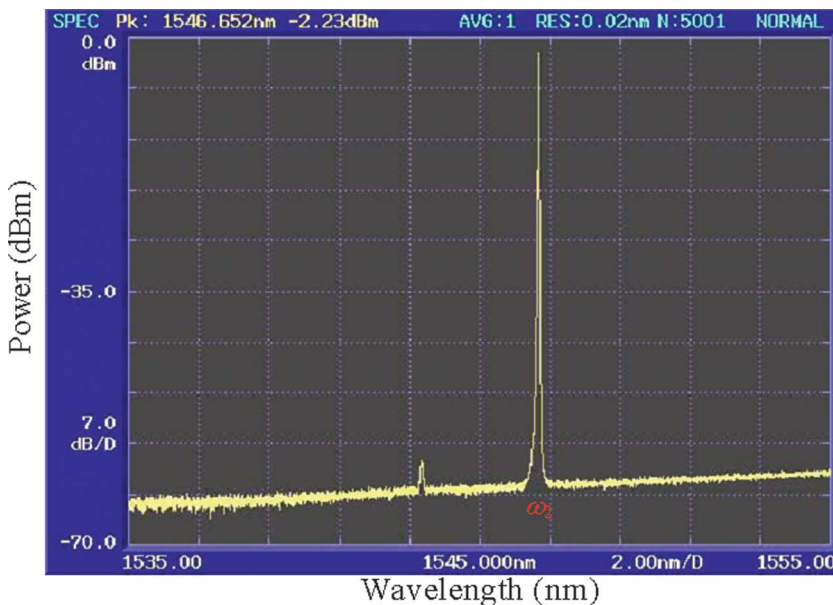
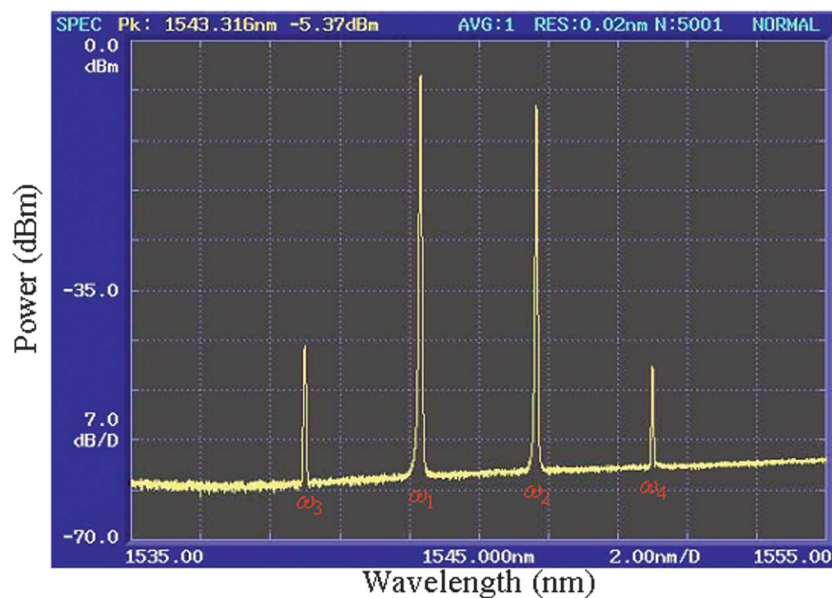
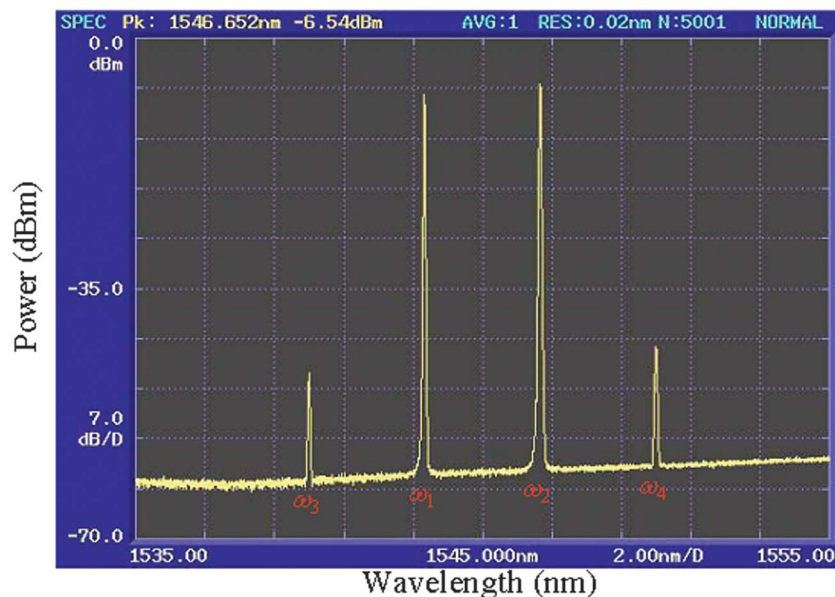


FIG. 4. (Color) Output power spectra without multiple FWM processes. The PCF is excluded in Fig. 2. Only a single wave of frequency  $\omega_2$  is stably lased by the EDF laser cavity.



(a)



(b)

FIG. 5. (Color) Output power spectra with the different reflection of FBG1 and FBG2 by adjusting VOA: (a)  $P_1 > P_2$  and (b)  $P_1 < P_2$ . The detailed descriptions are same as Fig. 3, except that two pump waves of  $\omega_1$  and  $\omega_2$  have different powers. If power  $P(\omega_1) > P(\omega_2)$ , then  $P(\omega_3) > P(\omega_4)$ , and vice versa.

waves at  $\omega_3$  and  $\omega_4$  are created by the FWM processes of PCF. Obviously, the powers of frequencies  $\omega_1$  and  $\omega_2$  are about four orders of magnitude larger than those of frequencies  $\omega_3$  and  $\omega_4$ . On the other hand, from Fig. 1(b) or Ref. [13], we can obtain that  $\Delta\beta_1 \approx \Delta\beta_2 \approx \Delta\beta_3 \approx 0$ , and  $(3\gamma P_1 - \Delta\beta_2)L \approx (3\gamma P_2 - \Delta\beta_1)L \approx 0.08$  (here,  $\gamma = 11 \text{ W}^{-1} \text{ km}^{-1}$ ,  $L = 51 \text{ m}$ , and  $P_1 \approx P_2 \approx 25 \text{ mW}$ ).<sup>1</sup> Therefore, two degenerate FWM processes (i.e.,  $2\omega_1 = \omega_2 + \omega_3$  and  $2\omega_2 = \omega_1 + \omega_4$ ) and one nondegenerate FWM process (i.e.,  $\omega_1 + \omega_2 = \omega_3 + \omega_4$ ) are

effectively interacted.

Experiments show that only a single wave of  $\omega_2$  is stably lased if without PCF in Fig. 2. The output spectra are illustrated in Fig. 4. In comparing Figs. 3 and 4, it can be seen that the self-stability effect of FWM processes plays the key factor to produce dual-wavelength EDF lasers in the experimental configuration of Fig. 2. Such a comparison has also verified the self-stability function of multiple FWM processes in experiments.

From Eq. (18), it is seen that, if  $P_1(0) > P_2(0)$ ,  $P_3(L) > P_4(L)$ , and vice versa. But  $P_3(L)/P_1(L) = P_4(L)/P_2(L)$ . Figure 5 demonstrates the experimental results, where Fig. 5(a) is for  $P_1(L) > P_2(L)$  and Fig. 5(b) is for  $P_1(L) < P_2(L)$ . The experiment results show the relationship of  $P_3(L)/P_1(L) \approx P_4(L)/P_2(L) \approx 37 \text{ dB}$ , which is consistent with the theoretical values.

<sup>1</sup>The experimental results show that the power of each laser in Fig. 3 is  $\sim 0.5 \text{ mW}$ . Taking into account the output power ratio of  $\sim 3\%$  and the total loss of  $\sim 1.7 \text{ dB}$  [e.g., connector loss between PCF and coupler, splicing loss of coupler, connecting loss between coupler and optical spectra analyzer (OSA), and some loss of jumpers], each laser power in the PCF is about  $25 \text{ mW}$ .

## V. DISCUSSIONS

This section aims at simplifying and verifying the coupled-mode equations in Eq. (9), and comparing to the traditional coupled-mode equations governing FWM processes. If  $|\Delta\beta_1|$  approaches zero and  $|\Delta\beta_3|$  and  $|\Delta\beta_2|$  in Eq. (9) are great, i.e., the phase mismatching in the latter is large, only the degenerate FWM of  $2\omega_1 = \omega_2 + \omega_3$  effectively occurs in the total nonlinear processes. The proof is as follows. When  $P_1 \gg P_3$  and  $P_2 \gg P_3$ , from Eq. (12d), we can achieve as

$$\begin{aligned} \sqrt{P_4} &= \int_0^L \gamma(P_2\sqrt{P_1}\sin\vartheta_2 + 2\sqrt{P_1P_2P_3}\sin\vartheta_3)dz \\ &\approx \int_0^L \gamma P_2\sqrt{P_1}\sin\vartheta_2 dz. \end{aligned} \quad (20)$$

Equation (2) shows that the power  $P_4$  of frequency  $\omega_4$  periodically evolves along the fiber distance  $z$  and its periodicity is determined by  $\Delta\beta_2$ . Integrating Eq. (20), one can obtain

$$P_4 < \gamma^2 P_2^2 P_1 / |\Delta\beta_2|^2. \quad (21)$$

From Eqs. (18) and (21), it is easily achieved as

$$P_3(L)/P_4(L) > L^2 |\Delta\beta_2|^2. \quad (22)$$

If  $|\Delta\beta_2| \gg 0$ ,  $P_3(t) \gg P_4(t)$  (here,  $L > 1$ ). Such a result has also been proved by experiments (see Fig. 6) and numerical solutions of Eq. (9). As a result, the terms including  $A_4$  (correspond to  $P_4$ ) in Eq. (9) can be reasonably ignored, and then Eq. (9) is simplified as

$$\frac{\partial A_1}{\partial z} = i\gamma_1[ (|A_1|^2 + 2|A_2|^2 + 2|A_3|^2)A_1 + 2A_1^*A_2A_3\exp(i\Delta\beta_1z)], \quad (23a)$$

$$\frac{\partial A_2}{\partial z} = i\gamma_2[ (|A_2|^2 + 2|A_1|^2 + 2|A_3|^2)A_2 + A_3^*A_1^2\exp(-i\Delta\beta_1z)], \quad (23b)$$

$$\frac{\partial A_3}{\partial z} = i\gamma_3[ (|A_3|^2 + 2|A_2|^2 + 2|A_1|^2)A_3 + A_2^*A_1^2\exp(-i\Delta\beta_1z)]. \quad (23c)$$

Similarly, if  $|\Delta\beta_2| \rightarrow 0$ ,  $|\Delta\beta_1| \gg 0$  and  $|\Delta\beta_3| \gg 0$ , we can achieve the coupled-mode equations for degenerate FWM of  $2\omega_2 = \omega_1 + \omega_4$  from Eq. (9), i.e.,

$$\frac{\partial A_2}{\partial z} = i\gamma_2[ (|A_2|^2 + 2|A_1|^2 + 2|A_4|^2)A_2 + 2A_2^*A_1A_4\exp(i\Delta\beta_2z)], \quad (24a)$$

$$\frac{\partial A_1}{\partial z} = i\gamma_1[ (|A_1|^2 + 2|A_2|^2 + 2|A_4|^2)A_1 + A_4^*A_2^2\exp(-i\Delta\beta_2z)], \quad (24b)$$

$$\frac{\partial A_4}{\partial z} = i\gamma_4[ (|A_4|^2 + 2|A_1|^2 + 2|A_2|^2)A_4 + A_1^*A_2^2\exp(-i\Delta\beta_2z)]. \quad (24c)$$

On the other hand, integrating Eq. (9d), we can get

$$\begin{aligned} A_4 &= \int_0^L i\gamma_4 \left[ (|A_4|^2 + 2 \sum_{j(\neq 4)} |A_j|^2)A_4 \right. \\ &\quad \left. + 2A_3^*A_1A_2\exp(-i\Delta\beta_3z) \right] dz \\ &\quad + \int_0^L i\gamma_4 A_1^*A_2^2\exp(-i\Delta\beta_2z) dz. \end{aligned} \quad (25)$$

If only the phase mismatching for nondegenerate FWM of  $\omega_1 + \omega_2 = \omega_3 + \omega_4$  vanishes and other phase matching is bad, i.e.,  $|\Delta\beta_3| \rightarrow 0$ ,  $|\Delta\beta_1| \gg 0$  and  $|\Delta\beta_2| \gg 0$ , the last term of Eq. (25) can be simplified as

$$\left| \int_0^L i\gamma_4 A_1^*A_2^2\exp(-i\Delta\beta_2z) dz \right| < |\gamma_4 A_1^*A_2^2 / \Delta\beta_2|. \quad (26)$$

Because of  $|\Delta\beta_2| \gg 0$ , Eq. (26) approaches zero, and then the terms involving  $\Delta\beta_2$  in Eq. (9) can be reasonably skimmed. Similarly, the terms including  $\Delta\beta_1$  in Eq. (9) can also be ignored. Thus, Eq. (9) can change as

$$\frac{\partial A_1}{\partial z} = i\gamma_1 \left[ (|A_1|^2 + 2 \sum_{j(\neq 1)} |A_j|^2)A_1 + 2A_2^*A_3A_4\exp(i\Delta\beta_3z) \right], \quad (27a)$$

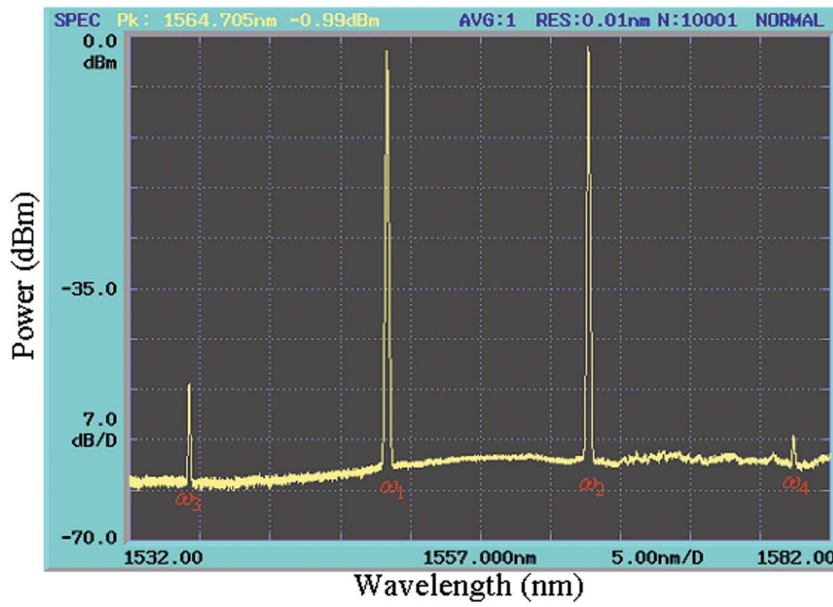
$$\frac{\partial A_2}{\partial z} = i\gamma_2 \left[ (|A_2|^2 + 2 \sum_{j(\neq 2)} |A_j|^2)A_2 + 2A_1^*A_3A_4\exp(i\Delta\beta_3z) \right], \quad (27b)$$

$$\frac{\partial A_3}{\partial z} = i\gamma_3 \left[ (|A_3|^2 + 2 \sum_{j(\neq 3)} |A_j|^2)A_3 + 2A_4^*A_1A_2\exp(-i\Delta\beta_3z) \right], \quad (27c)$$

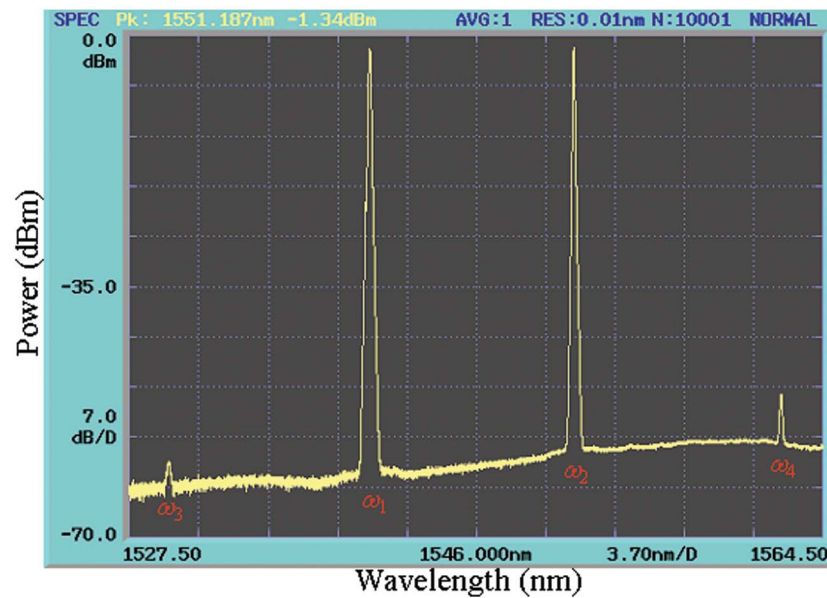
$$\frac{\partial A_4}{\partial z} = i\gamma_4 \left[ (|A_4|^2 + 2 \sum_{j(\neq 4)} |A_j|^2)A_4 + 2A_3^*A_1A_2\exp(-i\Delta\beta_3z) \right]. \quad (27d)$$

By comparing Fig. 1(a) to Fig. 1(b), it is shown that the dispersion property of PCFs is greatly different from that of traditional single-mode fibers. As a result, the model equations [i.e., Eqs. (23), (24), and (27)] in the conventional single-mode fibers will not be suitable to describe the nonlinear interacting mixing in the PCFs and the model and phenomena are covered in PCFs [8].

The key difference between our models and the conventional models for FWMs is that the former simultaneously involves three resonances while the latter only has one. To prove the fact that our models are more rigorous for describing FWM processes than the traditional models, Fig. 6 displays the experimental results. The experimental setup is the



(a)



(b)

FIG. 6. (Color) Output spectra for testifying multiple resonances simultaneously.  $\omega_1$  and  $\omega_2$  in (a) and (b) correspond to the zero-dispersion wavelength, respectively.

same with Fig. 2, except that the fiber Bragg gratings (FBGs) with differently central wavelengths replace FBG1 and FBG2 in Fig. 2. At the same time, PCF is replaced by a dispersion-shift fiber (DSF). The zero-dispersion wavelength of DSF is  $\sim 1551$  nm, the nonlinear coefficient  $\gamma$  is  $\sim 2/W/\text{km}$ , and the fiber length  $L$  is  $\sim 600$  m.

Figure 6 shows the output spectra for testifying multiple resonances simultaneously. Frequencies  $\omega_1$  and  $\omega_2$  in Figs. 6(a) and 6(b) correspond to the zero-dispersion wavelength, respectively. The conventional coupled-mode theory of FWM processes failed to explain the results of Fig. 6, if taking into account a single resonance. For example, if only the degenerate FWM process of  $2\omega_1 = \omega_2 + \omega_3$  occurs, the wave of frequency  $\omega_4$  in Fig. 6(a) should disappear. On the other hand, if only nondegenerate FWM process of  $\omega_1 + \omega_2 = \omega_3 + \omega_4$  occurs, the power  $P_3$  of frequency  $\omega_3$  should be approximately equal to  $P_4$  of frequency  $\omega_4$  in Figs. 6(a) and

6(b). Fortunately, our models can overcome these difficulties and explain the experimental results of Fig. 6. Figures 6(a) and 6(b) experimentally prove the fact that the double independence resonances are preferable to a single resonance in the FWM processes of both PCF and the conventionally optical fibers (e.g., DSF).

By comparing Fig. 3 to Fig. 6, it is seen that, although the power  $P_1$  of  $\omega_1$  is approximately equal to  $P_2$  of  $\omega_2$  in both PCF and DSF, the powers  $P_3$  and  $P_4$  at  $\omega_3$  and  $\omega_4$  are unequal in Fig. 6 rather than equal in Fig. 3. These significant differences originate from the dispersion performance and can be explained from Fig. 1 and Eq. (9). Because of  $\Delta\beta_1 \approx \Delta\beta_2 \approx \Delta\beta_3 \approx 0$  in PCF, the result of  $P_3 \approx P_4$  can be proven from the coupled equations of Eq. (9). However,  $\Delta\beta_1$ ,  $\Delta\beta_2$  and  $\Delta\beta_3$  in DSF are different. As a result,  $P_3 > P_4$  if  $\Delta\beta_1 \rightarrow 0$  [see Fig. 6(a)], and  $P_3 < P_4$  if  $\Delta\beta_2 \rightarrow 0$  [see Fig. 6(b)].

All of these results can be reasonably explained by our proposed theory.

## VI. CONCLUSIONS

In this paper, a model describing multiple FWM processes is investigated in the optical fibers, and the corresponding coupled-mode equations are derived. The propagation equations involve one nondegenerate and two degenerate FWM processes. The power conservation of four waves and their

energy flow relationship are obtained. Our proposed models are proved by the experiments, and are compared to the conventional coupled-mode theory of FWM processes. The analytic solutions show that the power flow between two pump waves is three times larger than that between two created waves [i.e., Eq. (14)], and that self-stability function is covered in these kinds of multiple FWM processes. On the basis of dual-wavelength EDF lasers, the self-stability effect is experimentally proven by clamping the mode competition of EDF. The achieved results can find a lot of applications in fiber lasers.

- 
- [1] H. Takesue and K. Inoue, *Phys. Rev. A* **70**, 031802 (2004).
  - [2] B. Khubchandani, P. N. Guzdar, and R. Roy, *Phys. Rev. E* **66**, 066609 (2002).
  - [3] G. Millot, *Opt. Lett.* **26**, 1391 (2001).
  - [4] S. O. Konorov, E. E. Serebryannikov, D. A. Akimov, A. A. Ivanov, M. V. Alfimov, and A. M. Zheltikov, *Phys. Rev. E* **70**, 066625 (2004).
  - [5] L. Deng and M. G. Payne, *Phys. Rev. Lett.* **91**, 243902 (2003).
  - [6] G. P. Agrawal, *Nonlinear Fiber Optics* (Academic, San Diego, 2001).
  - [7] G. Van Simaey, P. Emplit, and M. Haelterman, *J. Opt. Soc. Am. B* **19**, 477 (2002).
  - [8] F. Biancalana, D. V. Skryabin, and P. St. J. Russell, *Phys. Rev. E* **68**, 046603 (2003).
  - [9] N. I. Nikolov, T. Sørensen, O. Bang, and A. Bjarklev, *J. Opt. Soc. Am. B* **20**, 2329 (2003).
  - [10] A. V. Husakou and J. Herrmann, *J. Opt. Soc. Am. B* **19**, 2171 (2002).
  - [11] F. Benabid, G. Bouwmans, J. C. Knight, P. St. Russell, and F. Couny, *Phys. Rev. Lett.* **93**, 123903 (2004).
  - [12] K. L. Corwin, N. R. Newbury, J. M. Dudley, S. Coen, S. A. Diddams, K. Weber, and R. S. Windeler, *Phys. Rev. Lett.* **90**, 113904 (2003).
  - [13] (<http://www.crystal-fibre.com/datasheets/NL-1550-POS-1.pdf>)
  - [14] C. J. S. de Matos, S. V. Popov, A. B. Rulkov, J. R. Taylor, J. Broeng, T. P. Hansen, and V. P. Gapontsev, *Phys. Rev. Lett.* **93**, 103901 (2004).
  - [15] R. H. Stolen, J. E. Bjorkholm, and A. Ashkin, *Appl. Phys. Lett.* **24**, 308 (1974).
  - [16] G. Cappellini and S. Trillo, *J. Opt. Soc. Am. B* **8**, 824 (1991).
  - [17] J. R. Thompson and R. Roy, *Phys. Rev. A* **43**, 4987 (1991).
  - [18] A. N. Pisarchik, Yu. O. Barmenkov, and A. V. Kir'yanov, *Phys. Rev. E* **68**, 066211 (2003).
  - [19] Y. Z. Xu, H. Y. Tam, W. C. Du, and M. S. Demokan, *IEEE Photonics Technol. Lett.* **10**, 334 (1998).
  - [20] E. Desurvire, J. L. Zyskind, and J. R. Simpson, *IEEE Photonics Technol. Lett.* **2**, 246 (1990).
  - [21] E. Desurvire, C. Giles, and J. R. Simpson, *J. Lightwave Technol.* **7**, 2095 (1989).
  - [22] H. Okamura and K. Iwatsuki, *Electron. Lett.* **28**, 461 (1992).
  - [23] O. Graydon, W. H. Loh, R. I. Laming, and L. Dong, *IEEE Photonics Technol. Lett.* **8**, 63 (1996).
  - [24] J. Nilsson, Y. W. Lee, and S. J. Kim, *IEEE Photonics Technol. Lett.* **8**, 1630 (1996).